Available online at www.sciencedirect.com
SCIENCE DIRECT®
Journal of Chromatography A, 1052 (2004) 39–51
JOURNAL OF CHROMATOGRAPHY A
www.elsevier.com/locate/chroma

Effect of temperature in reversed phase liquid chromatography

D. Guillarme, S. Heinisch*, J.L. Rocca

Laboratoire des Sciences Analytiques, CNRS UMR 5180, Université Claude Bernard, 43 Bd du 11 Novembre 1918, 69622 Villeurbanne Cedex, France

Received 6 January 2004; received in revised form 28 July 2004; accepted 17 August 2004

Abstract

The high temperature liquid chromatography (HTLC) reveals interesting chromatographic properties but even now, it misses some theoretical aspects concerning the influence of high temperature on thermodynamic and kinetic aspects of chromatography: such a knowledge is very essential for method development. In this work, the effect of temperature on solute behavior has been studied using various stationary phases which are representative of the available thermally stable materials present on the market. The thermodynamic properties were evaluated by using different mobile phases: acetonitrile–water, methanol–water and pure water. The obtained results were discussed on the basis of both type of mobile phases and type of stationary phases. Type of mobile phase was found to play an important role on the retention of solutes. The kinetic aspect was studied at various temperatures ranging from ambient temperature to high temperature (typically from about 30 to 200 °C) by fitting the experimental data with the Knox equation and it was shown that the efficiency is improved significantly when the temperature is increased. In this paper, we also discussed the problem of temperature control for thermostating columns which may represent a significant source of peak broadening: by taking into account the three main parameters such as heat transfer, pressure drop and band broadening resulting from the preheating tube, suitable rules are set up for a judicious choice of the column internal diameter.

Keywords: High temperature liquid chromatography; Kinetic and thermodynamic behavior; Temperature control

1. Introduction

HPLC analysis are usually carried out at ambient or just above ambient temperature. By working at higher temperatures, it is possible to improve the analysis conditions because some physical parameters playing an important role in HPLC, such as viscosity, mobile phase polarity or diffusivity depend strongly on the temperature. Some years ago, some authors studied the influence of temperature on chromatographic separations, but the temperature range of interest was usually from ambient temperature up to 60 °C: only a few studies were devoted to very high temperatures [1–5]. Nowadays, high temperature liquid chromatography (HTLC) is known to provide very attractive improvements compared to classical HPLC [6]: it allows a reduction of the organic content in the mobile phase and provides faster separations without loss of efficiency. Furthermore, the use of temperature as separation parameter in order to improve selectivity can be used very successfully [7–9]. The major drawback of the column high temperature is the risk of stationary phase degradation and consequently classical bonded silicas which are largely thermally unstable have to be used very carefully. Development of new generation of silica based columns [10,11] as well as nonsilica based ones, much more thermally stable, will offer the possibility to carry out high temperature experiments without major damage of column packing.

HTLC analysis requires efficient equipment in order to heat the column at the required temperature without radial temperature gradients inside the column [12,13], as they are known to involve excessive band broadenings. In order to prevent them, mobile phase preheating is of main importance. The heat exchanger is placed in an oven either prior to or after the injection valve. In the first case, the injection valve has to resist to high temperatures, meanwhile in the second case, additional band broadening has often a significant effect on

* Corresponding author. Tel.: +33 4 72 44 82 17; fax: +33 4 72 43 10 78.
E-mail address: heinisch@univ-lyon1.fr (S. Heinisch).

0021-9673/$ – see front matter © 2004 Elsevier B.V. All rights reserved.
doi:10.1016/j.chroma.2004.08.052

the separation quality. A new technology [14] has been recently developed. It consists in heating the tubing walls by applying a voltage under microprocessor control, resulting in a significant reduction of the required tubing length. In most cases, mobile phase preheating is performed by plunging the preheating tube into the column bath which may represent an important limitation to HTLC especially when an air circulation oven is used. It was shown [15] that peak efficiencies with water or oil baths are much higher than with an air bath since heat transfers into a liquid are much better and band broadenings reduced. However, it is obvious that an air system is much more functional than an oil bath for many reasons: firstly, temperature variations are dramatically faster with an air system, secondly, one of the great interests of HTLC is the possible coupling with a flame ionization detector which is easy with the oven of the classical GC-FID system and thirdly, temperature programming is very difficult with an oil bath. Yet, temperature programming may represent an interesting alternative technique to gradient elution for micro or nano columns since it eliminates the problem of the delay volume. A recent study [16] showed that it was possible to use an air system at low flow-rates (1 ml min^{-1}) only, provided that the eluent was heated up to 80 °C. In fact, the preheater tubing must be long enough to avoid thermal mismatch broadening and short enough to avoid extra-column broadening. By comparing the tubing lengths required for an efficient preheating of the mobile phase at high flow-rates and/or at high temperatures [16] when air bath or silicone bath were used, it was concluded that air bath would lead to excessive extra-column broadenings with a tubing length seven-fold longer. In contrast, other authors found [17] that a 1.5 m long preheater tubing is appropriate at 200 °C with flow-rates up to 3 ml min^{-1}. Recently [16], it was shown that with an oil bath, narrow bore columns (2.1 mm i.d.) gave better thermal equilibration of the eluent compared to wider bore columns (4.6 mm i.d.). But it seems that no systematic study has been performed to identify exactly the limitation of the air system, according to both column diameter and temperature. Furthermore, some authors [18–20] worked at high temperature without any preheating of the mobile phase. In this work we studied the possibilities of the air system in HTLC taking into account the only three relevant parameters: required length of tubing, pressure drop into the tubing and peak band broadening due to the solute dispersion into the preheating tube.

The knowledge of the chromatographic behavior of solutes at high temperatures is essential to develop methods in HTLC. Various studies have contributed to prove the great advantages of using high temperatures and many interesting applications especially with hot water as mobile phase [21–23] have been shown; a few studies [9,24,25] have investigated the kinetic and thermodynamic aspects of HTLC. Unfortunately, these studies were generally performed on a unique type of stationary phase and/or within a limited range of temperature and/or with a unique type of mobile phase. The goal of the present work is to study the behavior of various stationary phases, various mobile phases within a large interval of temperatures in order first to obtain a global overview of the effect of temperature and then to compare the behavior of conventional stationary phases such as new silica based materials to new generations of stationary phases such as polymeric, graphitic carbon or zirconia based materials.

2. Theoretical

2.1. Dependence of column efficiency on temperature

The column efficiency is commonly given by the plate number, N, which is related to the plate height, H, by $N = L_{col}/H$, L_{col} being the column length. H varies with the linear velocity of mobile phase, u, and its variation may be expressed by the Van Deemter equation [26].

By using reduced parameters h and ν defined by $h = H/d_p$ and $\nu = ud_p/D_m$, d_p being the average particle diameter and D_m the molecular diffusion coefficient of the solute in the mobile phase, Knox developed the following well-known equation [27]:

$$h = A\nu^{1/3} + \frac{B}{\nu} + C\nu \quad (1)$$

The A term depends on both the quality of the column packing and the contribution of slow mass transfer across the moving stream. The B term accounts for longitudinal diffusion. The C term expresses the effect of mass transfer resistances in both stagnant mobile phases and stationary phases. In case of low ν values, the second contribution (B/ν) of the Knox equation is predominant whereas the third term $C\nu$ becomes predominant in case of high ν values. Theoretically, for terms A–C invariant with the temperature, there should be only one plot h versus ν, independent on the temperature. In fact, both B and C terms depend on solute retention [27] and consequently, for a given solute and a given mobile phase, they should depend on temperature since the retention decreases when the temperature increases. While the B term is usually said to be roughly independent on the temperature [24], the variation of both A and C terms with temperature is largely discussed. It has been found that the reduced plate height, h_{opt}, at the optimum reduced velocity (ν_{opt}) decreased with temperature [24,28–30], increased with temperature [31,32] or was roughly invariant with temperature [3,33,34]. A decrease of column efficiency (increase in h_{opt}) with temperature was often attributed to extra-column band broadening which of course has a higher effect on low solute retentions corresponding to high temperatures. It was also attributed to the negative impact of temperature due to thermal gradients that may exist inside the column when the eluent temperature at the column inlet is different from the temperature of the column walls. Both problems can easily be overcome: the first one by minimizing the importance of extra-column dispersion (lower extra-column variance value, higher k value), the second one by using an efficient preheating of the mobile

phase (see next section). On the other hand, some authors have noted an increase of column efficiency (decrease in h_{opt}) with temperature [33]. This phenomenon was attributed to slow kinetic systems where an increase in temperature may improve the mass transfer resistance and consequently decrease the C term. Furthermore, the kinetics of secondary interactions, which are often responsible of peak tailings are probably accelerated at elevated temperature, eliminating the tailing.

The plot of h versus ν requires the estimation of the diffusion coefficients which is not a simple task. This estimation may be obtained either from experimental measures of the peak standard deviation of a solute placed into a long tube filled with the desired solvent at the desired temperature [35,36] or from empirical equations such as the widely used Wilke–Chang equation [37]. This equation is given by:

$$D_{A,B} = 7.4 \times 10^{-8} \frac{(\Phi_B M_B)^{1/2} T}{\eta_B V_A^{0.6}} \quad (2)$$

where $D_{A,B}$ is the diffusion coefficient of solute A at very low concentration in solvent B ($cm^2\,s^{-1}$), M_B the molecular weight of solvent B ($g\,mol^{-1}$), T the absolute temperature (K), η_B the viscosity of solvent B (cP) at T, V_A the molar volume of solute A at its normal boiling temperature ($cm^3\,g^{-1}\,mol^{-1}$) and ϕ_B, is the association factor of solvent B (dimensionless). Wilke and Chang recommended a value of ϕ at 2.6 when the solvent was water, at 1.9 when the solvent was methanol and at 1.0 when the solvents are unassociated (for example, acetonitrile). It was later found that the predictions were more accurate if the value of ϕ was reduced to 2.26 for organic solutes diffusing into water [38]. Some authors [36] found up to 30% differences when comparing the diffusion coefficients computed from the Wilke–Chang equation and their experimental values. For the diffusion coefficient of a solute in an homogeneous mixed solvents, Eq. (2) can be used with the association parameter redefined as [38]:

$$\Phi M = \sum_{j=1}^{n} x_j \Phi_j M_j \quad (3)$$

where x_j is the mole fraction of solvent j, ϕ_j, its association parameter and M_j, its molecular weight.

2.2. Temperature control in HTLC with an air circulation oven

Three parameters are relevant to evaluate the possibilities of a preheating system: the required tube length, L_{tube}, the contribution of the preheating tube to peak dispersion, σ^2_{tube} (partial peak variance) and the pressure drop into the tube, ΔP_{tube}, the preheating performance being hardly affected by the tube diameter [3], provided that the tube wall is thin and the thermal resistance to heat transfer through the tube wall is small.

Thompson et al. [16] used the convenient following equation based on theoretical considerations to calculate L_{tube}:

$$L_{tube} = \dot{m} C_p R'_{th} \ln\left(\frac{T_{in} - T_{oven}}{T_{out} - T_{oven}}\right) \quad (4)$$

where $\dot{m}$ is the mass flow-rate of the mobile phase, C_P, its mean specific heat, T_{oven}, the oven temperature. T_{in} and T_{out} are the eluent temperature at the preheating tube inlet and outlet, respectively, R'_{th} represents the total resistance to heat transfer. It has been shown [16], in case of an air bath, that this term depends essentially on the resistance to convective heat transfer from the air bath to the outer wall of the preheating tube. As a result, it depends both on the convective heat transfer coefficient of the forced air which varies according to the convection rate and on the outer diameter of the tube. The higher the heat transfer coefficient and/or the outer diameter, the smaller the resistance to transfer. According to [3,13,15], even when T_{oven} differed from T_{out} of 5 °C, no significant thermal broadenings were observed. Since $\dot{m} = \rho F$, F being the mobile phase flow-rate and ρ, its density, Eq. (4) can be changed in:

$$L_{tube} = \rho F C_p R'_{th} \ln\left(\frac{T_{in} - T_{oven}}{T_{out} - T_{oven}}\right) \quad (5)$$

F being given by

$$F = \frac{u_{col} \varepsilon \pi d_{col}^2}{4} \quad (6)$$

where u_{col} is the linear velocity of the mobile phase through the column, d_{col} the column diameter and ε is the total column porosity. As shown by Eqs. (5) and (6), L_{tube} is proportional to F and then proportional to d^2_{col}.

The pressure drop into the tubing, with the required L_{tube}, can be expressed by the Poiseuille–Hagen expression dedicated to a laminar flow system:

$$\Delta P_{tube} = 128 \frac{\eta L_{tube} F}{\pi d^4_{tube}} \quad (7)$$

For a given temperature T_{oven}, with a desired difference between T_{oven} and T_{out} (for example, 5 °C), a given column and a given mobile phase, u_{col} (optimum linear velocity for example), C_p, η, ε and ρ are fixed. Furthermore, R'_{th} is fixed for a given preheating system (for example, forced air) and a given outer diameter tubing. By replacing in Eq. (7) F and L_{col} by the relationships given in Eqs. (5) and (6), respectively, the pressure drop inside the tubing becomes directly proportional to $(d_{col}/d_{tube})^4$ as follows:

$$\Delta P_{tube} = K_1 \frac{d^4_{col}}{d^4_{tube}} \quad (8)$$

K_1 being the proportionality constant given by

$$K_1 = 8\eta\rho\varepsilon^2\pi C_p R'_{th} u^2_{col} \ln\left(\frac{T_{in} - T_{oven}}{T_{out} - T_{oven}}\right) \quad (9)$$

The maximum acceptable pressure drop inside the tubing, $\Delta P_{\text{tube,max}}$ (for example, 20–30 bars representing 10% of the maximum pressure of the solvent delivery system), will then fix the minimum value for d_{tube}^4 according to:

$$K_1 \frac{d_{\text{col}}^4}{\Delta P_{\text{tube,max}}} \leq d_{\text{tube}}^4 \tag{10}$$

The peak variance σ_{peak}^2, is the sum of variances due to external (σ_{ext}^2) and internal (σ_{col}^2) contributions, respectively. Usually, the external variance is expected to be less than 10% of the internal one in order to loose less than 9% of the column efficiency. If all the external variances (detector and injector contributions) have been minimized except the tubing variance (σ_{tube}^2), the following relationship should be applied:

$$\frac{\sigma_{\text{tube}}^2}{\sigma_{\text{col}}^2} \leq 0.1 \tag{11}$$

σ_{tube}^2 [39] and σ_{col}^2, are respectively given by:

$$\sigma_{\text{tube}}^2 = \frac{d_{\text{tube}}^4 L_{\text{tube}} F}{122 D_{\text{m}}} \tag{12}$$

and

$$\sigma_{\text{col}}^2 = \frac{V_{\text{r}}^2}{N} = \frac{L_{\text{col}}^2 \pi^2 \varepsilon^2 (1+k)^2}{16N} \times d_{\text{col}}^4 \tag{13}$$

where N is the column plate number and k, the solute retention factor.

As previously discussed, for given conditions of temperature, column, mobile phase, solutes and preheating system, u_{col}, C_{p}, ε, D_{m}, ρ, $R_{\text{th}}^{'}$, L_{col}, N and k are fixed. By replacing in Eq. (12) F and L_{tube} by the relationships given in Eqs. (5) and (6), respectively and by considering Eq. (13), it appears that $\sigma_{\text{tube}}^2/\sigma_{\text{col}}^2$ becomes directly proportional to d_{tube}^4 according to:

$$\frac{\sigma_{\text{tube}}^2}{\sigma_{\text{col}}^2} = K_2 d_{\text{tube}}^4 \tag{14}$$

K_2 being the proportionality constant given by

$$K_2 = \frac{\rho C_{\text{p}} R_{\text{th}}^{'} N u_{\text{col}}^2}{122 D_{\text{m}} L_{\text{col}}^2} \tag{15}$$

Eq. (11) becomes

$$d_{\text{tube}}^4 \leq \frac{0.1}{K_2} \tag{16}$$

Considering Eqs. (8) and (16), it appears that the preheating can be achieved under acceptable conditions of pressure and extra-column band broadenings when:

$$d_{\text{col}}^4 \leq 0.1 \times \frac{K_1}{K_2} \times \Delta P_{\text{tube,max}} \tag{17}$$

According to Eq. (17), it is obvious that column miniaturization is the most reliable way to overcome all problems of preheating.

2.3. Effect of temperature on retention properties

The influence of temperature on solute retention factor, k, is a function of the free energy changes in the interaction between the solute and the stationary phase according to the following expression (Van't Hoff equation):

$$\log k = -\frac{\Delta H_0}{2.3RT} + \frac{\Delta S_0}{2.3R} + \log \Phi \tag{18}$$

where ΔH_0 and ΔS_0 are the system enthalpy and entropy, T the absolute temperature, R the universal gas constant and Φ is the phase ratio of the system. For neutral solutes, the plot of $\log k$ versus $1/T$, also called Van't Hoff plot, is usually linear with a slope of $-\Delta H_0/2.3R$ and an intercept of $\Delta S_0/2.3R + \log \Phi$ provided that ΔH_0 and ΔS_0 are invariant with temperature [40,41]. Many authors [24,42] observed linear Van't Hoff plots with hydro organic mobile phases for temperature ranges of about 90 °C. Some small deviations from linearity were observed [43–46] and attributed to the so-called "phase transition" phenomenon. That is the consequence of a change in the molecular structure of the stationary phase which appears in the 20–50 °C range for C18 silica based stationary phases. This phenomenon is quite independent on the nature of both solute and eluent. However, it was shown that these deviations were relevant only for stationary phases with high bonding density [45,46] (bonding densities higher than 4.0 μmol/m^2).

Curvilinear Van't Hoff plots were more rarely observed [47]. However, Hearn and Zhao [48] studied the dependency of $\ln k$ on T for several polypeptides with acetonitrile–water mixtures and methanol–water mixtures on a *n*-butyl silica stationary phase and found nonlinear Van't Hoff plots for temperatures ranging from 278 to 358 K, with acetonitrile–water mixtures. They related the classical linear Van't Hoff behavior to a change in the heat capacity of the system independent on T (case of methanol–water mixtures) and the nonclassical Van't Hoff behavior to a change in the heat capacity dependent on T (case of acetonitrile–water mixtures). In this case, both ΔH_0 and ΔS_0 vary with T according to the following relationships:

$$\ln k = b_0 + \frac{b_1}{T} + \frac{b_2}{T^2} + \ln \Phi \tag{19}$$

with

$$\Delta H = -R\left(b_1 + \frac{2b_2}{T}\right) \tag{20}$$

and

$$\Delta S = R\left(b_0 - \frac{b_2}{T^2}\right) \tag{21}$$

where b_0, b_1 and b_2 are the coefficients to be determined.

Another expression was given to express $\ln k$ versus $1/T$ in case of nonlinear Van't Hoff curves [49] as follows:

$$\ln k = A + \frac{B}{T} + C \ln T \tag{22}$$

where A–C are the coefficients to be determined.

It was shown in the case of proteins [50], that the change in the system pressure induced by a change in the column temperature can mask or alter the true temperature influence on k. In fact, this problem can be easily overcome only if experimental data are acquired at constant pressure in place of at constant flow-rate.

Until now, as most silica based phases are thermally unstable and can only be used at temperatures not higher than 60–80 °C, just a few investigations have been performed within a wide temperature range (from ambient up to 200 °C). A study of $\log k$ versus $1/T$ within such a range and with various mobile and stationary phases has not been reported yet.

3. Experimental

3.1. Instrument

The HTLC system (Fig. 1) consisted in two Shimadzu LC10AD pumps, a Perkin-Elmer auto system GC oven equipped with a temperature controller, a Shimadzu SPD6A spectrophotometer detector set at 254 nm with either a 8 μL high pressure cell (case of classical 4.6 mm i.d. columns) followed by a Jasco 880-81 system maintained at a constant back pressure of 50 bars or a 0.5 μl cell with a fused silica capillary (50 μm i.d. columns) placed before the detector to maintain the mobile phase in the liquid state (1 mm i.d. columns). The time constant of the detector was set at 0.1 s. In case of classical 4.6 mm i.d columns, the injection valve was a Rheodyne model 7125 (3 μl sample loop), in case of 1 mm i.d columns, the injection valve was a Rheodyne model 7520 (0.5 μl sample loop). A preheating tube was placed into the oven between the injection valve and the column. The length has been adapted to both the flow-rate and the temperature according to the results obtained and discussed into the Section 4. The mobile phase was continuously degassed with nitrogen for oxygen elimination to avoid corrosion problems. The oven temperature was continuously controlled with a thermometer. The temperature of the eluent entering into the column was measured at the end of the preheating tube with a type T copper–constantan thermocouple. It was assumed that the temperature of the eluent was equal to the surface temperature at the outside of the tube. This assumption is justified by the low resistance to conductive heat transfer throughout a thin metallic tube. About five centimeters of the thermocouple sonde were tied with the end of the preheating tube and overlaid with thermal insulation in order to insulate it against the oven temperature.

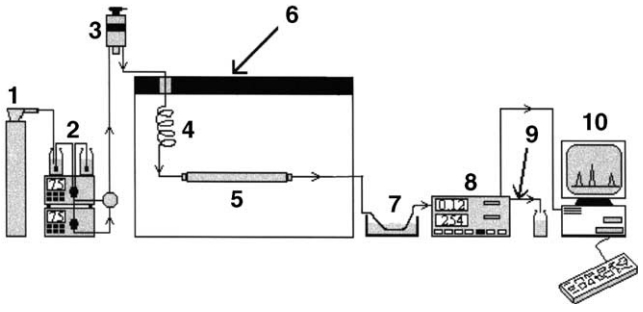

Fig. 1. Scheme of the HTLC system: 1, nitrogen for purging the mobile phase; 2, pumps; 3, injection valve; 4, preheating coil; 5, column; 6, GC oven; 7, cooling bath; 8, UV detector; 9, tube for back pressure 18 cm × 100 μm; 10 computerized data acquisition system.

The acquisition data were processed with the Azur acquisition software (Datalys, France). The acquisition frequency was set at 10 or 20 Hz depending on the flow-rate.

3.2. Viscosity measurements

The viscosities of aqueous acetonitrile or methanol mixtures as a function of T were obtained from the experimental data of the total backpressure using a Zirchrom-DB-C18 column, thermally stable. The pressure measurements were performed using the chromatographic instrument previously described. The eluent mixtures were prepared in the range 0–100% (v/v) by hand mixing. The eluent was pumped at 2ml min^{-1} through a 50 mm × 4.6 mm column packed with 3 μm particles, placed into the oven, followed by a 100 μm i.d. fused silica capillary at room temperature with an adequate length to maintain a column outlet pressure higher than the vapor pressure of the solvent. The pressure drop into the capillary was measured and deduced from the total pressure drop of the system.

3.3. Analytical columns

Different stationary phases were studied:

1 Zirchrom-PBD (3 μm, 50 mm × 4.6 mm i.d.) from Zirchrom separations (Anoka, USA).
2 Zirchrom-DB-C18 (3 μm, 50 mm × 4.6 mm i.d.) from Zirchrom separations (Anoka, USA).
3 PLRP-S (5 μm, 150 mm × 4.6 mm i.d.) from Polymer Laboratories (Church Stretton, UK).
4 MS-Xterra-C18 (5 μm, 150 mm × 4.6 mm i.d.) from Waters (Milford, USA).
5 RP-Xterra-C18 (5 μm, 150 mm × 4.6 mm i.d.) from Waters (Milford, USA).
6 Nucleodur-C18 (3 μm, 70 mm × 4.6 mm i.d.) from Macherey Nagel (France).
7 Kromasil-C18 (5 μm, 150 mm × 4.6 mm i.d.) from Thermo electron (France).
8 Hypercarb (5 μm, 100 mm × 4.6 mm i.d.) and (5 μm, 100 mm × 1 mm i.d.), both from Hypersil (France).

Columns were selected in order to have a wide representation of the different thermally stable packings: both Zirchrom packing are zirconia based. The Zirchrom-PDB is obtained by deposition and cross-linking of polybutadiene on the surface of zirconia [51]. The Zirchrom-DB-C18 is obtained by chemical vapor deposition of hydrocarbons on porous zirconia [52]. The Nucleodur-C18 and Kromasil-C18 are C18

bonded silicas while the MS-Xterra C18 and RP-Xterra C18 are hybrid C18 bonded silicas. The Hypercarb is made of porous graphitic carbon and the PLRP-S is an organic polymer (polystyrene divinylbenzene type).

3.4. Materials and reagents

Water was distilled and deionised. Acetonitrile (MeCN) and methanol (MeOH) were of HPLC grade from SDS (Peypin, France). All the solutes used in this study were of high purity from Sigma–Aldrich (France).

4. Results and discussion

4.1. Temperature control using an air circulation oven

A comprehensive experimental study has been performed to determine the required length as a function of both temperature and flow-rate using an air circulation oven. Various lengths of stainless steel tubings ranging from 1 to 5.50 m were tested as preheaters for the incoming solvent, in our air circulation oven. These tubes had outer diameter of 1/16″ (1.59 mm) and internal diameter of 0.005″ (0.127 mm). Zirchrom-DB-C18 as column and water as eluent were used in these experiments. Flow-rates were varied from 1 to 10 ml min^{-1} and the temperature from 100 to 200 °C. These conditions of flow-rates were adapted to classical column diameters (4.6 mm i.d.). The outlet temperature was measured with the thermocouple at the end of the tube before the eluent enters into the column. Measured temperatures were compared to the oven temperature and the differences are reported in Fig. 2. In most cases, one or two meter tubing lengths have been proved to be long enough for a suitable preheating (a difference $T_{oven} - T_{out}$ value lower than 5 °C). At 200 °C with flow-rates higher than 5 ml min^{-1}, longer tubes were required. With a 10 ml min^{-1} flow-rate, a tube of 4 m long was required. Our determined lengths of stainless steel tubings are higher than those calculated in [16] but as said

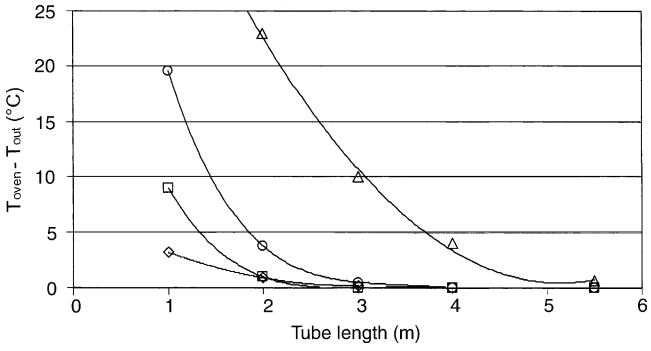

Fig. 2. Experimental measured differences in temperature between the incoming eluent and the oven as a function of the stainless steel tube length for different oven temperatures and mobile phase flow-rates: (◊): 100 °C and 3 ml min^{-1}; (□): 150 °C and 4 ml min^{-1}; (○): 200 °C and 5 ml min^{-1}; (△): 200 °C and 10 ml min^{-1}.

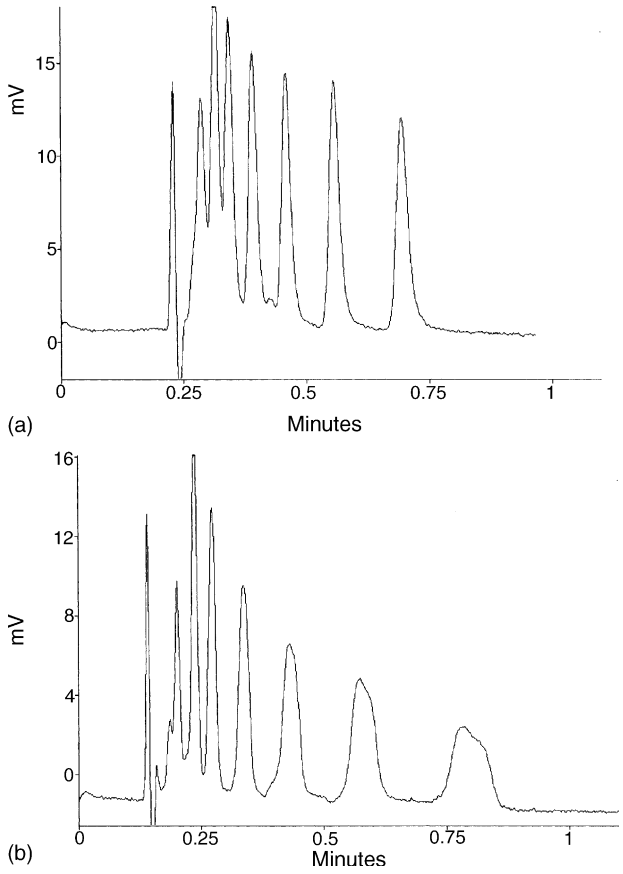

Fig. 3. Chromatograms showing the effect of an efficient (a) and inefficient (b) preheating on the peak shape, solutes: benzene, toluene, ethylbenzene, propylbenzene, butylbenzene, pentylbenzene, column Zirchrom-DB-C18 4.6 mm i.d. 50 mm length, flow-rate 4 ml min^{-1}, temperature 150 °C, i.d preheating tube 127 mm, length preheating tube 2 m (a) and 1 m (b).

previously, these lengths are dependent on the total resistance to heat transfer (R'_{th}) which varies according to the air convection rate and differs from oven to oven. Fig. 3 shows the effect of an inadequate preheating on the separation of alkylbenzenes at 150 °C with a flow-rate of 4 ml min^{-1}. One meter of tubing is definitely inappropriate meanwhile 2 m provide good peak shapes.

As the required length is directly proportional to F (Eq. (5)), it is possible, from our results, to calculate the required length for any column diameter (Eq. (6)) using a linear velocity adapted to the temperature. It can be pointed out that the tubing length also depends on R'_{th} and this term is roughly inversely proportional to the outer diameter of the tube [3] when the heat transfer coefficient is assumed to be independent on the outer diameter. The outer diameter depends on whether the tube is stainless steel (1.6 mm o.d.) or fused silica (0.375 mm o.d.). For a given flow-rate F and a given tube outer diameter $d_{o,tube}$ (expressed in mm), the required tube length is then given by:

$$L_{tube} = L_{tube,ref} \frac{F}{F_{ref}} \frac{1.6}{d_{o,tube}} \quad (23)$$

Table 1
Calculated ΔP_{tube} and $\sigma^2_{tube}/\sigma^2_{col}$ for four column internal diameters at 100 and 200 °C in water

Temperature (°C)	Viscosity[a] (cP)	D_m ($\times 10^{-5}$ cm^2 s^{-1})	u (mm s^{-1})	Column i.d. (mm)	4.6	2.1	1	0.32
				Preheating tube i.d. (μm)	127	100	75	50
				Preheating tube o.d. (mm)	1.6	0.375	0.375	0.375
				σ^2_{col} (μl^2) (Eq. (13))	1082	47	2	0.025
30	1	1	1	F (μl min^{-1}) (Eq. (6))	700	145	33	3
100	0.30	4.1	4	F (μl min^{-1}) (Eq. (6))	2863	597	135	14
				L_{tube}(cm)	100[b]	90	18	0.4
				σ^2_{tube} (μl^2) (Eq. (12))	10*	0.7	0.01*	0.000004
				$(\sigma^2_{tube}/\sigma^2_{col}) \times 100$	1	1.5	0.4	0.0
				ΔP_{tube} (bars) (Eq. (7))	22*	11	2*	0.02
200	0.15	10.4	10	F (μl min^{-1}) (Eq. (6))	7260	1513	343	35
				L_{tube}(cm)	400[b]	360	70	1.5
				σ^2_{tube} (μl^2) (Eq. (12))	103*	7	0.1*	0.00004
				$(\sigma^2_{tube}/\sigma^2_{col}) \times 100$	10	16	4.5	0.2
				ΔP_{tube} (bars) (Eq. (7))	114*	55	10*	0.1

Calculations were obtained from Eqs. (5)–(7), (12) and 13 using the following values: L_{col} = 100 mm, N = 5000 plates, ε = 0.7, k = 1, $D_m = 1 \times 10^{-5}$ cm^2 s^{-1} at 30 °C in water and $u_{optimum}$ = 1 mm s^{-1} at 30 °C. See text for more explanations.
[a] From ref. [38].
[b] Experimental values given by Fig. 2.

where $L_{tube,ref}$ is the tube length reported on Fig. 2 for the flow-rate, F_{ref}, leading to a difference $T_{oven} - T_{out}$ lower than 5 °C. Using Eqs. (7), (12) and (13), it is possible to calculate ΔP_{tube}, σ^2_{tube} and σ^2_{col}, assuming that η and D_m keep constant values all along the total length of the heating tube, and corresponding to values obtained at T_{out}. This assumption is consistent as the eluent temperature increases exponentially with the distance from the tube inlet and as a result the viscosity decreases exponentially. Table 1 lists the values calculated at 100 and 200 °C for four different usual column diameters, 4.6, 2.1, 1 and 0.320 mm. Tube length values for 4.6 mm i.d. column are those reported on Fig. 2. The internal diameters of the preheating tubes were chosen among the commercially available tubes in order to provide the best compromise between a low ΔP_{tube} value and a low $\sigma^2_{tube}/\sigma^2_{col}$ value. Viscosities values were found in the Perry's [38] for water as solvent. The diffusion coefficients D_m were estimated by assuming $D_m \approx 1 \times 10^{-5}$ cm^2 s^{-1} for acetone at 30 °C in water and the relationship $D_m \propto T/\eta$ (from Wilke–Chang equation Eq. (2). The linear velocities, u, were estimated by assuming $u_{optimum} \approx 1$ mm s^{-1} at 30 °C and the relationship $u_{optimum} \propto D_m$.

Some experimental measurements of ΔP_{tube} and σ^2_{tube} were carried out with acetone as solute and they were found to be close to the calculated ones (within 30%) (asterisked in Table 1). It appears that at 200 °C, with column diameters of 4.6 and 2.1 mm, at optimum linear velocities, both ΔP_{tube} and $\sigma^2_{tube}/\sigma^2_{col}$ are higher than the maximum allowed values (30 bars and 10%, respectively). It means that it is impossible to find an internal diameter of tube providing acceptable values of both ΔP_{tube} and $\sigma^2_{tube}/\sigma^2_{col}$, and as a consequence, any preheating conditions are unsatisfactory. For all other conditions, both ΔP_{tube} and $\sigma^2_{tube}/\sigma^2_{col}$ values are lower than the allowed values and there is even no need for mobile phase preheating when using a 0.32 mm internal column. This study brings us to the conclusion that an air system is fully adapted to HTLC up to 200 °C. This technique can be applied to classical column (4.6–2.1 mm i.d.) with temperatures up to 150 °C and flow-rates lower than 4 ml min^{-1}. In contrast, we found no limitation for the utilization of an air system when using micro columns (1 mm i.d. or less) at higher temperatures.

4.2. Effect of temperature on column efficiency

Up to now, very few datas are available on viscosity of mixed binary eluents. Existing data often concern either temperatures ranging from low temperatures up to 60 °C [53], or pure solvents at temperatures up to 200 °C [38]. However, Chen and Horvath [54] established the following empirical relationship to determine the viscosity of aqueous acetonitrile mixtures at various temperatures ranging from ambient up to 120 °C:

$$\eta_{\Phi,T} = \exp\left[\Phi\left(-3.476 + \frac{726}{T}\right) + (1-\Phi)\left(-5.414 + \frac{1566}{T}\right) + \Phi(1-\Phi)\left(-1.762 + \frac{929}{T}\right)\right] \quad (24)$$

When comparing calculated values using Eq. (24) and experimental values, Thompson and Carr [55] concluded that this correlation was good to within ±20% from 100 to 200 °C.

We also made an attempt to determine viscosity values for aqueous methanol and aqueous acetonitrile mixtures, by using the method described into the experimental section. The measured pressure drops were obtained at different temperatures, T, varying from 25 to 200 °C and with different eluent

Table 2
Values of viscosity (cP) obtained according to method described in experimental section and used to calculate the correlations 26 and 27

T (°C)	Methanol in mobile phase (%)						Acetonitrile in mobile phase (%)					
	0	20	40	60	80	100	0	20	40	60	80	100
25[a]	0.89	1.4	1.62	1.54	1.12	0.56	0.89	0.98	0.89	0.72	0.52	0.35
60	0.53	0.68	0.74	0.72	0.60	0.35	0.53	0.59	0.55	0.52	0.43	0.31
90	0.38	0.44	0.45	0.47	0.42	0.26	0.39	0.40	0.39	0.38	0.34	0.24
140	0.21	0.23	0.25	0.22	0.18	0.13	0.26	0.26	0.24	0.24	0.24	0.18
180	0.3	0.13	0.14	0.13	0.13	0.10	0.19	0.21	0.21	0.21	0.20	0.15

[a] From reference [53].

compositions ϕ ranging from 0 to 100% of organic solvent. These values allow an evaluation of the viscosity $\eta_{T,\phi}$ by means of the Darcy's law according to:

$$\eta_{T,\Phi} = \frac{\Delta P_{T,\Phi}}{\Delta P_{25\,^\circ\mathrm{C},\Phi}} \times \eta_{25\,^\circ\mathrm{C},\Phi} \tag{25}$$

where $\Delta P_{T,\phi}$ and $\Delta P_{25\,^\circ\mathrm{C},\phi}$ are the measured pressure drops with the eluent composition ϕ and at temperatures T and 25 °C, respectively; $\eta_{25\,^\circ\mathrm{C},\phi}$ is the eluent viscosity at 25 °C determined by Colin et al. [53]. It was assumed of course that the specific permeability is independent on the temperature. At the end of such experiments, pressure drops were measured once more time at 25 °C in order to verify that the specific permeability did not vary all along the different experiments. Our viscosity values (Table 2) obtained with this method were correlated using a polynomial regression. The following relationships were obtained:

$$\eta_{\Phi,T} = 10^{(-2.429+(0.714/T)-1.859\Phi+(0.9117\Phi/T)+1.8586\Phi^2-0.9681(\Phi^2/T))} \tag{26}$$

for aqueous methanol mixtures and

$$\eta_{\Phi,T} = 10^{(-2.063+(0.6019/T)+0.0709\Phi+(0.062\Phi/T)+0.5043\Phi^2-0.3458(\Phi^2/T))} \tag{27}$$

for aqueous acetonitrile mixtures.

Both equations provide a good fitting of the viscosity values with a difference between determined and calculated values within ±10%. Our calculated values were compared to viscosity values given in the literature. The differences with those given by [53] at 60 °C were within ±10% for aqueous methanol mixtures and ±20% for aqueous acetonitrile mixtures. Furthermore, the calculated values for aqueous acetonitrile mixtures were compared to those given by Eq. (24), and the differences were within ±5% at low temperature and up to 25% at 180 °C.

The diffusion coefficients of a solute A, $D_{A,\phi,T}$, at a temperature, T, into a given solvent, ϕ, were estimated by using the following convenient equation, derived from the Wilke–Chang equation (Eq. (2)) and based on experimental values of the diffusion coefficient at 30 °C into a solvent B.

$$D_{A,\Phi,T} = \frac{(\Phi M)_\Phi^{1/2} T}{\eta_{\Phi,T}} \times \frac{\eta_{B,30\,^\circ\mathrm{C}}}{(\Phi M)_B^{1/2} \times 303} \times D_{A,B,30\,^\circ\mathrm{C}} \tag{28}$$

Experimental values of the diffusion coefficients at 30 °C were taken from [36] for alkylbenzenes and [35] for other solutes.

Reduced plate heights (h) versus reduced linear velocity (ν) were plotted for four different stationary phases at different temperatures (Figs. 4–7). Experimental values were fitted with the Knox equation (Eq. (1)). For the Hypercarb, PLRP-S and Zirchrom-DB-C18 stationary phases, all experiments have been performed with the same k value by decreasing the organic modifier content in the mobile phase while increasing temperature. As shown in the previous section, it is better to use micro columns (1 or 0.32 mm i.d.) at very high temperatures but it was more convenient for this study to use classical ones (4.6 mm i.d.). In all cases, preheating tube lengths were calculated in order to provide adequate preheating of the mobile phase according to Fig. 2, despite high pressure drops or high external variances. However, in order to account for the extra-column dispersion, column plate numbers N were calculated according to the following relationship:

$$N = \frac{(t_r - t_{ext})^2}{(\sigma^2_{total} - \sigma^2_{ext})} \tag{29}$$

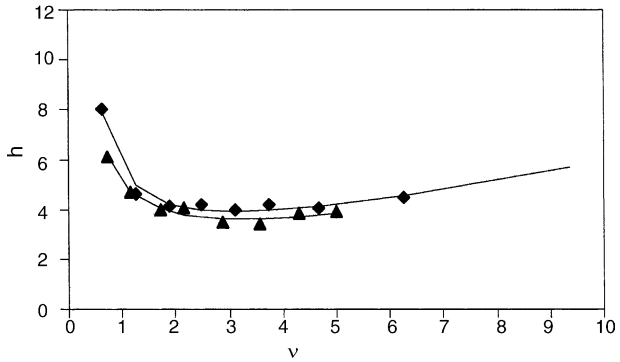

Fig. 4. Reduced plate height vs. linear velocity at various temperatures, column Nucleodur 75 mm × 4.6 mm, solute propylbenzene, mobile phase water–acetonitrile 35:65 v/v; (♦) 30 °C (k = 5); (▲) 90 °C (k = 2.3).

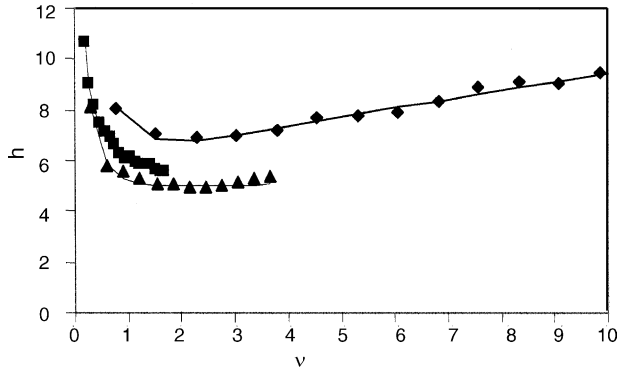

Fig. 5. Reduced plate hight vs. linear velocity at various temperatures, column PLRP-S 150 mm × 4.6 mm, solute methyl parahydroxybenzoate (k = 1), (♦) 30 °C, water–acetonitrile 50:50 v/v; (▲) 90 °C, water–acetonitrile 65:35 v/v; (■) 200 °C, water–acetonitrile, 90:10 v/v.

where t_r is the solute retention time, t_{ext} the external time spent by the solute in the preheating tube that is negligible in most cases, σ^2_{total} and σ^2_{ext} is the total peak variance and the external variance, respectively, expressed in time units. σ^2_{ext} was obtained from the calculation of statistical moment (order 2) of a peak produced without column; σ^2_{total} was calculated from the measurement of the peak width at half peak height, all the chosen solutes providing symmetrical peaks (asymmetry factor lower than 1.2 and higher than 0.9).

The plots of h versus ν show that the optimum reduced linear velocity (ν_{opt}) is totally independent on the temperature for all the studied stationary phase. Consequently, the optimum linear velocity (u_{opt}) will always increase proportionally to the solute diffusion coefficient and as a result, according to the Wilke–Chang relationship, it will increase proportionally to T/η. It may be concluded that HTLC improves drastically analysis speed (5–15-fold from ambient up to 200 °C depending on the increase in η). According to the Darcy's law, the column backpressure at the optimum linear velocity will then vary proportionally to T (for example, for a given mobile phase, the column backpressure at 200 °C will be 1.6 times higher (ratio 473/293) than at 20 °C). Thus, as it is not commonly expected, HTLC is not appropriate for

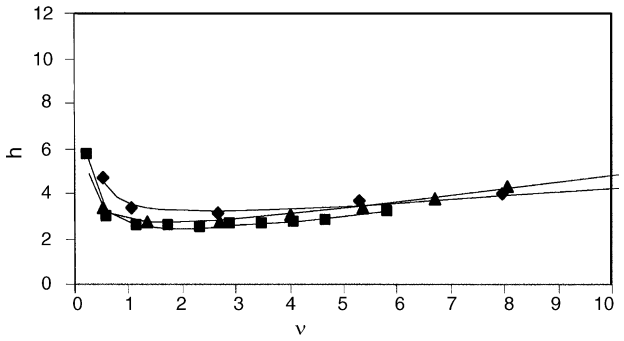

Fig. 6. Reduced plate height vs. linear velocity at various temperatures,column Hypercarb 100 mm × 4.6 mm, solute fenuron, (♦) 25 °C, methanol, k = 4.5; (▲) 60 °C, methanol, k = 3; (■) 100 °C, water–methanol 30:70 v/v, k = 3.

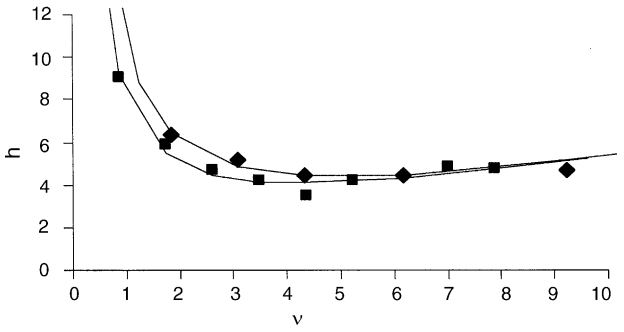

Fig. 7. Reduced plate height vs. linear velocity at various temperatures, column Zircone DB-C1850 mm × 4.6 mm, solute propylbenzene (k = 10); (♦) 30 °C, water–acetonitrile 50:50 v/v; (■) 180 °C, water–acetonitrile 90:10 v/v.

reducing column backpressures (at the optimum linear velocity) and therefore it does not make the use of particle size smaller than the conventional ones (5–3 μm) easier.

It is very interesting to note that the optimum reduced plate height (h_{opt}) decreased with temperature for all studied stationary phases, and particularly for PLRP-S stationary phase. It can be assumed that this reduction is coming from the reduction of the mass transfer resistance which is often more relevant in the case of polymeric materials. No concomitant significant change in the C term has been highlighted but our explored ν range was obviously not large enough at high temperature to discuss C variations with temperature. On the other hand, significant improvements in some peak shapes have been found at high temperatures as shown in the chromatograms of Figs. 8 and 9 which represent the separation of caffeine derivatives on a zirchrom-DB18 column and a Hypercarb column, respectively. Peak tailings can result from secondary interactions the sorption/desorption kinetics of which being increased with temperature. These separations show the great improvement in analysis speed when using high temperatures. The dead time, indeed, is reduced to only 6 s on Fig. 9b. Since the calculated plate number is about 7000, it appears that the plate number per time unit (N/t_m) reaches a very high value, close to 1200 plates/s, which is impossible to get at ambient temperature even with monolithic columns. In addition, the corresponding backpressures read on the pump system are given on figure captions. These values were obviously very high with classical columns (Fig. 8) due to the significant required tubing length, thus confirming the beneficial effect of small i.d. columns in HTLC (Fig. 9).

4.3. Dependence of the retention on temperature

The variations of log k as a function of $1/T$ were studied for the different columns described into the experimental section with different mobile phases and for various neutral solutes. Figs. 10–13 show the resulting Van't Hoff plots. These plots were fitted either with a linear model (resultant correlation coefficient r^2 higher than 0.995) or with a quadratic model. In this case, all the fitting curves were obtained with $r^2 > 0.998$.

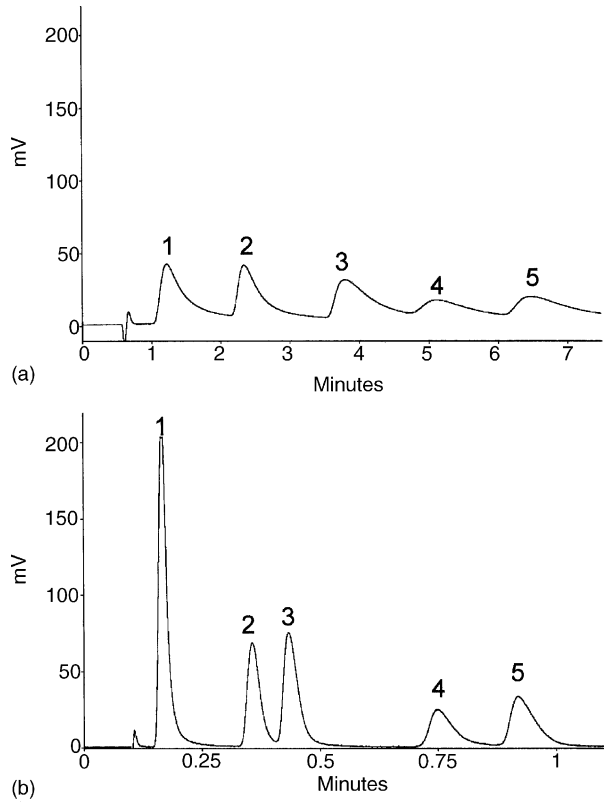

Fig. 8. Effect of temperature on the separation of caffeine derivatives (1, hypoxantine; 2, theobromine; 3, theophilline; 4, caffeine; 5, β-hydroxy-ethyl-theophilline), column Zirchrom-DB-C18 4.6 mm i.d. 50 mm length, 254nm UV detection, 300 ng injected, (a) 25 °C, 1 ml min^{-1}, water–methanol 60:40 v/v, backpressure resulting from tubing and column 40 bars (b) 150 °C, 7 ml min^{-1}, water, 2 m × 0.127 mm preheating tube, backpressure resulting from tubing and column 300 bars.

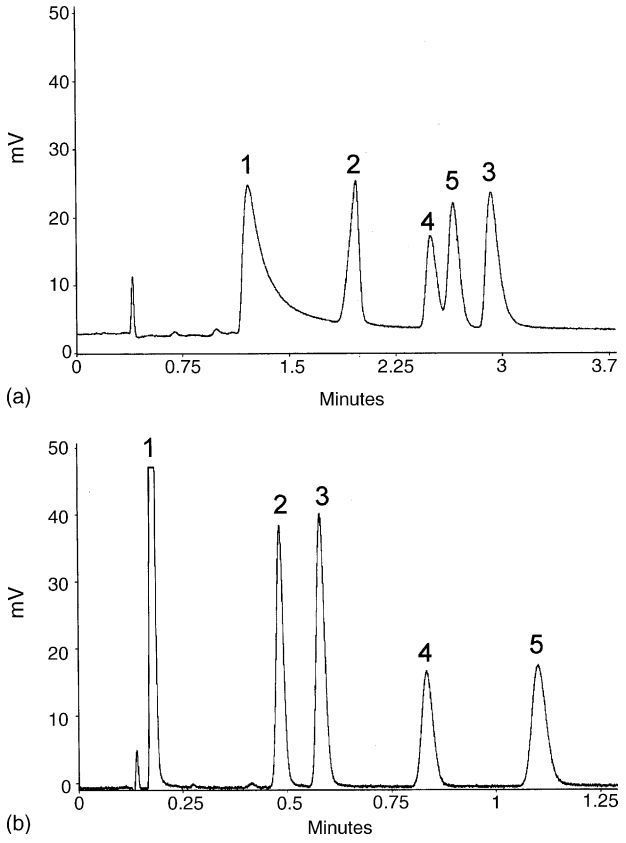

Fig. 9. Effect of temperature on the separation of caffeine derivatives (same solutes as Fig. 8 column Hypercarb 1 mm i.d. 100 mm length, 254 nm UV detection, 50 ng injected, (a) 100 °C, 200 μl min^{-1}, acetonitrile, 1 m × 100 μm preheating tube, backpressure resulting from tubing and column 90 bars, (b) 180 °C, 500 μl min^{-1}, water–acetonitrile 70:30 v/v, 1 m × 100 μm preheating tube, backpressure resulting from tubing and column 180 bars.

It is interesting to note that for all the Van't Hoff plots with all types of stationary phases, the data can be considered as linear within a narrow temperature range 25–80 °C. Within a larger range of temperature, a quadratic model is often required. We have observed that this behavior is totally independent on the nature of the solute but is dependent on both types of stationary and mobile phases.

Linear relationships of log k versus $1/T$ for the different studied silica based columns are given on Fig. 10. The linearity of the curves concerns all types of, aqueous–acetonitrile and aqueous–methanol mobile phases. However, the studied range of temperature was not very wide (20–100 °C) due to the thermal instability of silica based columns. We can conclude that within this range of temperature, the classical linear relationship can be applied with a very good approximation in a view to method development. On Fig. 11 are shown the plots of log k versus $1/T$ for the Hypercarb column. Although the range of temperature is much wider (20–180 °C), the linear relationship provides a very good fit of the experimental data, suggesting that with the Hypercarb column ΔH and ΔS are essentially temperature-independent over the entire examined temperature range, whatever the mobile phase composition is, even with pure water. In contrast, for the PLRP-S (Fig. 12a and b), when using aqueous–acetonitrile mixtures, it appears that the shapes of the Van't Hoff plots are quite different from those obtained with aqueous methanol mixtures. With the first eluents, the curves are clearly quadratic whereas they are quite linear with the second eluents. Linear Van't Hoff plots are usually reported with some rare exceptions [49] for low molecular weight organic compounds. In

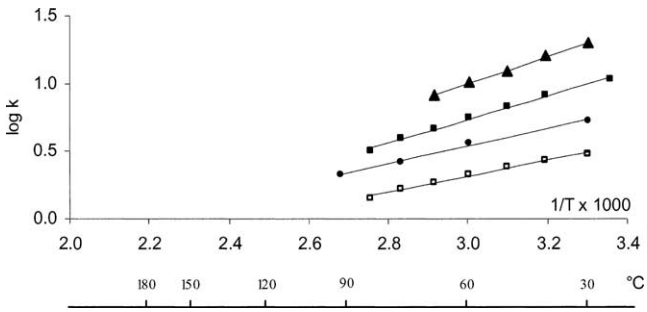

Fig. 10. Plot of log k vs. $1/T$ for silica based stationary phases; (●) Kromasil C18 with methanol–water 55–45 v/v, solute benzene; (■) MS-Xterra C18 with acetonitrile–water 30–70 v/v, solute propylparaben; (□) RP-Xterra C18 with acetonitrile–water 60-40 v/v, solute propylbenzene; (▲) Nucleodur C18 Gravity with acetonitrile–water 5–95 v/v, solute phenol.

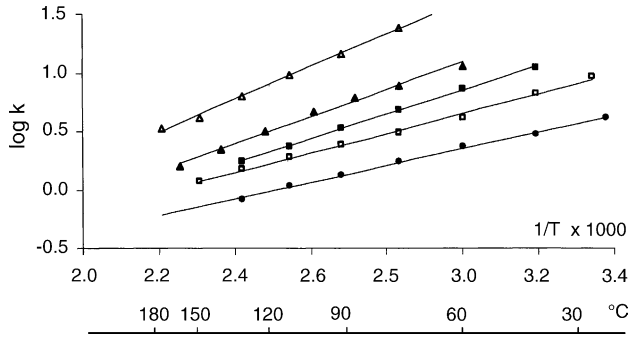

Fig. 11. Plot of log k vs. $1/T$ for Hypercarb column, (●) with methanol, solute fenuron; (■) with methanol–water 70–30 v/v, solute fenuron; (□) with acetonitrile–water 30–70 v/v, solute benzene as solute; (▲) with water, solute benzene; (△) with water, solute hexanol.

contrast, curvilinear Van't Hoff plots were observed by Hearn and Zhao [48] for high molecular weight solutes (polypeptides) on *n*-butylsilica over a range of T from 278 to 358 K: this behavior was also reported with acetonitrile–water and not with methanol–water eluents. Explanations were given as difference in molecular organization between the two organic solvents, hydrogen bonding interactions being more efficient with methanol than with acetonitrile. It was concluded that the nonclassical behavior was influenced by the nature of the organic solvent in solvent–water mixtures. From the above results, it is obvious that the nature of the stationary phase also influences the Van't Hoff plot characteristics, as it is seen

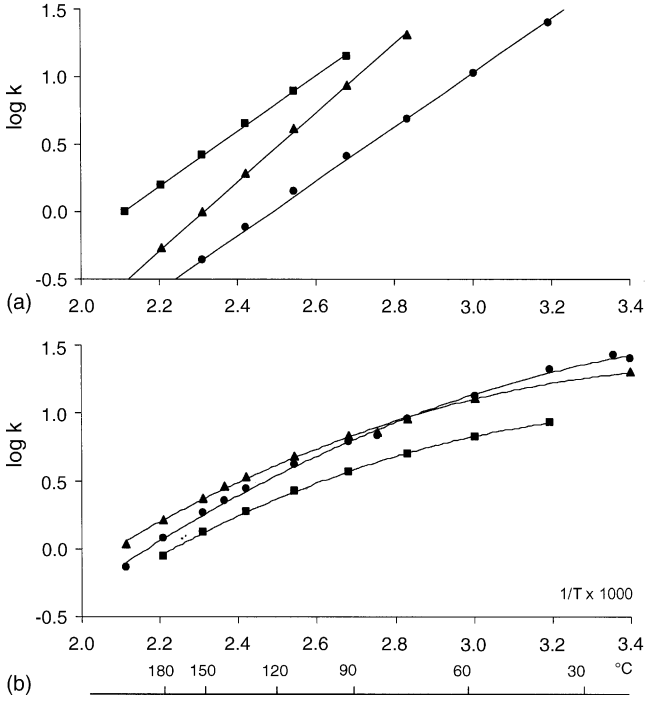

Fig. 12. Plot of log k vs. $1/T$ for the PLRP-S column, (a) with water–methanol mobile phases; (▲) 50–50 v/v, solute m-toluidine; (●) 50–50 v/v, solute ethylparaben; (■) 60–40 v/v, solute benzene, (b) with water–acetonitrile mobile phases; (▲) 80–20 v/v, solute m-toluidine; (●) 80–20 v/v, solute ethylparaben; (■) 60–40 v/v, solute benzene.

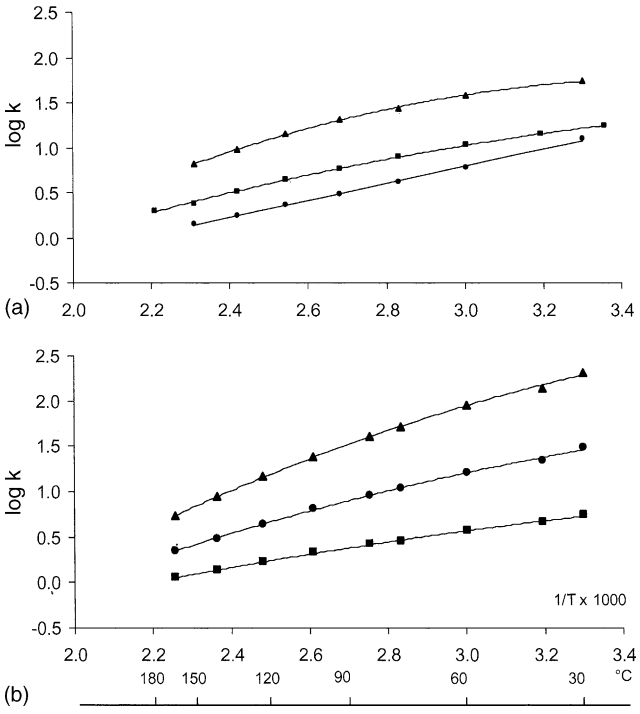

Fig. 13. Plot of log k vs. $1/T$ for zirconia based stationary phases. (a) Zirchrom-DB-C18 solute benzene; (■) with water–acetonitrile 80–20 v/v; (▲) with water; (●) with water–methanol 60–40 v/v, (b) Zirchrom-PDB with water–acetonitrile 80–20 v/v; (■) solute benzene; (●) solute ethylbenzene; (▲) solute butylbednzene; (□) RP-Xterra C18 with water–acetonitrile 40–60 v/v, solute propylbenzene; (▲) Nucleodur C18 gravity with water–acetonitrile 95–5 v/v, solute phenol.

on log k versus $1/T$ curves of Fig. 13a and b. Hence curvilinear Van't Hoff plots arise with acetonitrile–water eluents for all studied solutes and for both zirconia based stationary phases. On the other hand, the Van't Hoff plots are always linear with methanol–water eluents. It is also interesting to note the curvilinear Van't Hoff plot with pure water, despite the hydrogen bonding interaction behavior of such a solvent, and the contradiction with the explanations previously given.

As pointed out by some authors [50], this nonclassical Van't Hoff behavior might be attributed to changes in the system backpressure with temperature which should result in an alteration of the true temperature dependence of k. We have therefore compared the Van't Hoff curves of Fig. 13a obtained at constant flow-rate, resulting in a change of backpressure as a function of temperature with curves obtained in the same conditions of mobile phase but at constant backpressure of 110 bars, resulting in a change in flow-rate. In fact, quite identical quadratic curves were observed, proving that the quadratic profile was not resulting from pressure variations.

Another explanation could be that the surface of the stationary phase is more or less modified by the temperature in the presence of the solvent, this modification of the surface being unlikely with Hypercarb due to its perfect regularity and rigidity. In contrast, it may be more likely on PLRP-S as this material is well known to swell as a function of tem-

perature and as a function of the type and percent of organic solvent.

Anyway, for neutral solutes, existing in an unique form, nonlinear Van't Hoff behavior is probably resulting from a change in the mechanism of retention. From a practical point of view, it was noticed that a linear model is no more valid as soon as the studied range of temperature is too wide (wider than 100 °C): it is clearly observed, on the first one hand with water–methanol used as mobile phase rather than with water–acetonitrile, and on the second hand with hypercarb and bonded silicas rather than with organic polymer and zirconia. For retention prediction with a view to method development, it is undoubtedly better to use the quadratic model in all cases when the range of temperature is larger than 100 °C. Considering the slopes of the Van't Hoff curves, it appears that k decreases about 1–3% every °C depending on the solute, on the stationary phase and on the mobile phase. It means that an increase of 30–50 °C plays quite the same effect on retention as an increase of 10% of organic modifier in binary hydroorganic mobile phases at ambient temperature. The use of high temperatures greatly reduces the percent of organic solvent in the mobile phase as shown by the separation of caffeine derivatives (Figs. 8 and 9). In both Figs. 8 and 9 (Zirchrom-DB-C18) and (Hypercarb), the eluent strength of the mobile phase is quite the same (same range of k values) for the chromatograms a and b while the percent of organic solvent decreases from 40% at 25 °C (Fig. 8a) to 0% at 150 °C (Fig. 8b) and from 100% at 100 °C (Fig. 9a) to 30% at 180 °C (Fig. 9b).

5. Conclusions

This study demonstrates that it is quite possible to use an air system in HTLC under conditions of temperature: either up to 150 °C with classical i.d. columns or up to 200 °C with 1 mm or less i.d. columns.

It was shown that for all the studied stationary phases, an increase in column temperature improves significantly the performances of the chromatographic separation:

- Increase of the analysis speed (5–15 times higher when temperature is increased from ambient temperature up to 200 °C).
- Increase of column efficiency by decrease of the optimum reduced plate height (h_{opt}) with temperature, particularly when organic polymers such as PLRP-S are used as stationary phases.
- Improvement of peak symmetry due to limitation of secondary interactions.

Nonlinear Van't Hoff behavior was observed in case of acetonitrile–water mixtures or pure water used as mobile phases. In constrast, linear Van't Hoff behavior was observed with Hypercarb used as stationary phase, whatever the organic solvent (methanol or acetonitrile) of the binary mobile phase. Such a behavior difference is still not explained. Therefore, for retention predictions in the view to method development, it is undoubtedly better to use a quadratic relationship to express $\log k$ as a function of $1/T$ mainly for wide range of temperature higher than 100 °C.

References

[1] I.D. Wilson, Chromatographia 52 (2000) 28.
[2] R.M. Smith, R.J. Burgess, Anal. Commun. 33 (1996) 327.
[3] B. Yang, J. Zhao, J.S. Brown, J. Blackwell, P.W. Carr, Anal. Chem. 72 (2000) 1253.
[4] Y. Yang, A.D. Jones, C.D. Eaton, Anal. Chem. 71 (1999) 3808.
[5] S.B. Hawthorne, Y. Yang, D.J. Miller, Anal. Chem. 66 (1994) 2912.
[6] B. Ooms, LC GC Int. 9 (1996) 574.
[7] P.L. Zhu, J.W. Dolan, L.R. Snyder, J. Chromatogr. A 756b (1996) 41.
[8] S. Goga-Remont, S. Heinisch, E. Lesellier, J.L. Rocca, A. Tchapla, Chromatographia 51 (2000) 536.
[9] J. Li, Anal. Chim. Acta 369 (1998) 21.
[10] A. Tchapla, C. Stella, S. Rudaz, J.L. Veuthey, A. Tchapla, Chromatographia 53 (2001) 113.
[11] Y. Yang, LC GC Europe 6 (2003) 5.
[12] H. Chen, Cs. Horváth, J. Chromatogr. A 705 (1995) 3.
[13] R.G. Wolcott, J.W. Dolan, L.R. Snyder, R. Bakalyar, M.A. Arnold, J.A. Nichols, J. Chromatogr. A 869 (2000) 211.
[14] B. Jones, S.J. Marin, J. Clark, D. Felix, International Symposium on High Performance Liquid Phase Separations and Related Technologies, Nice, France, 2003.
[15] H. Poppe, J.C. Kraak, J. Chromatogr. 282 (1983) 399.
[16] J.D. Thompson, J.S. Brown, P.W. Carr, Anal. chem. 73 (2001) 3340.
[17] S.M. Fields, C.Q. Ye, D.D. Zhang, B.R. Branch, X.J. Zhang, N. Okafo, J. Chromatogr. A 913 (2001) 197.
[18] D.J. Miler, S.B. Hawthorne, Anal. Chem. 69 (1997) 623.
[19] B.A. Ingelse, H.G. Janssen, C.A. Cramers, J. High Resolut. Chromatogr. A 21 (1998) 613.
[20] Y. Yang, A.D. Jones, J.A. Mathis, M.A. Francis, J. Chromatogr. A 942 (2002) 231.
[21] T. Teutenberg, O. Lerch, H.J. Gotze, P. Zinn, Anal. Chem. 73 (2001) 3896.
[22] R.M. Smith, R.J. Burgess, O. Chienthavorn, J.R. Stuttard, LC GC Int. (1999) 30.
[23] R.M. Smith, R. Burgess, J. Chromatogr. A 785 (1997) 49.
[24] J. Li, P.W. Carr, Anal. Chem. 69 (1997) 837.
[25] C.B. Castells, P.W. Carr, Chromatographia 52 (2000) 535.
[26] J.J. van Deemter, F.J. Zuiderweg, A. Klinkenberg, Chem. Eng. Sci. 5 (1958) 271.
[27] G.J. Kennedy, J.H. Knox, J. Chromatogr. Sci. 10 (1972) 549.
[28] P. Molander, R. Trones, K. Haugland, T. Greibrokk, Analyst 124 (1999) 1137.
[29] J.S. Yoo, J.T. Watson, V.L. Mc Guffin, J. Microcolumn Sep. 4 (1992) 349.
[30] G. Herbut, J. Kowalczyk, J. High Resolut. Chromatogr. 4 (1981) 27.
[31] F.V. Warren, B.A. Bidlinmeyer, Anal. Chem. 60 (1988) 2824.
[32] T.S. Kephart, P. Dasgupta, Anal. Chim. Acta 414 (2000) 71.
[33] F.D. Antia, Cs. Horváth, J. Chromatogr. 435 (1988) 1.
[34] G. Liu, N.M. Djordjevic, F. Erni, J. Chromatogr. 592 (1992) 239.
[35] Z. Sahraoui, Thesis, Lyon, France, 1987.
[36] J. Li, P.W. Carr, Anal. Chem. 69 (1997) 2530.
[37] C.R. Wilke, P. Chang, AICHE J. 1 (1955) 264.
[38] Perry's Chemical Engineer's Handbook, McGraw, 1984.
[39] R.P.W. Scott, P. Kucera, J. Chromatogr. Sci. 9 (1971) 641.
[40] L.A. Cole, J.G. Dorsey, Anal. Chem. 62 (1990) 16.
[41] A. Tchapla, S. Heron, H. Colin, G. Guiochon, Anal. Chem. 60 (1988) 1443.

[42] T. Takeuchi, Y. Watanabe, D. Ishii, J. High Resolut. Chromatogr. 4 (1981) 300.
[43] A. Nahum, C. Horvath, J. Chromatogr. 203 (1981) 53.
[44] S. Heron, Thesis, Paris, 1992.
[45] D. Morel, J. Serpinet, J. Chromatogr. 214 (1981) 202.
[46] L.A. Cole, J.G. Dorsey, Anal. Chem. 64 (1992) 1317.
[47] L.A. Cole, J.G. Dorsey, k.A. Dill, Anal. Chem. 64 (1992) 1324.
[48] M.T.W. Hearn, G. Zhao, Anal. Chem. 71 (1999) 4874.
[49] Y. Mao, P.W. Carr, Anal. Chem. 72 (2000) 110.
[50] P. Szabelski, A. Cavazzini, K. Kaczmarski, X. Liu, J. Van Horn, G. Guiochon, J. Chromatogr. A 950 (2002) 41.
[51] M.P. Rigney, T.P. Weber, P.W. Carr, J. Chromatogr. 484 (1989) 273.
[52] T.P. Weber, P.T. Jackson, P.W. Carr, Anal. Chem. 67 (1995) 3042.
[53] H. Colin, J.D. Diez-Masa, G. Guiochon, J. Chromatogr. 167 (1978) 41.
[54] H. Chen, C. Horvath, Anal. Methods Instrum. 1 (1993) 213.
[55] J.D. Thompson, P.W. Carr, Anal. Chem. 74 (2002) 4150.